Journal of Medicinal Chemistry

Brief Article

pubs.acs.org/jmc

Peptide Truncation Leads to a Twist and an Unusual Increase in Affinity for Casitas B-Lineage Lymphoma Tyrosine Kinase Binding Domain

Eric A. Kumar,[†,●] Ziyan Yuan,[†,●] Nicholas Y. Palermo,[†] Lin Dong,[†] Gulzar Ahmad,[†] G. L. Lokesh,[●] Carol Kolar,[†] Smitha Kizhake,[†,●] Gloria E. O. Borgstahl,[†,‡] Hamid Band,[†,§,∥,⊥,#,∞] and Amarnath Natarajan*[,†,‡,§,●]

[†]Eppley Institute for Research in Cancer and Allied Diseases, Departments of [‡]Pharmaceutical Sciences, [§]Genetics, Cell Biology and Anatomy, [∥]Biochemistry and Molecular Biology, [⊥]Pathology and Microbiology, and [#]Pharmacology and Experimental Neuroscience, and [∞]College of Medicine, University of Nebraska Medical Center, Omaha, Nebraska 68022, United States

[●]Chemical Biology Program, Department of Pharmacology, University of Texas Medical Branch, Galveston, Texas 77555, United States

Supporting Information

ABSTRACT: We describe truncation and SAR studies to identify a pentapeptide that binds Cbl tyrosine kinase binding domain with a higher affinity than the parental peptide. The pentapeptide has an alternative binding mode that allows occupancy of a previously uncharacterized groove. A peptide library was used to map the binding site and define the interface landscape. Our results suggest that the pentapeptide is an ideal starting point for the development of inhibitors against Cbl driven diseases.

INTRODUCTION

The casitas B-lineage lymphoma (Cbl) family of proteins plays a fundamental role in controlling tyrosine kinase-coupled cellular signaling pathways. A family of multidomain proteins that functions as scaffold-type E3 ubiquitin ligases, Cbl proteins specialize in negatively regulating activated protein tyrosine kinases (PTKs).[1−5] The Cbl−PTK interaction is a phosphorylation driven event that involves direct interaction between the N-terminal tyrosine kinase binding domain (TKB) of Cbl with cognate phosphotyrosyl peptide motifs on PTKs.[6,7] The E3 ubiquitin ligase activity is mediated by the RING finger domain adjacent to the TKB domain. A highly conserved linker region bridges the TKB and the RING domains and participates with the RING finger in physical interactions with E2 ubiquitin conjugating enzymes (UBCs).[8] Within the C-terminal half, a proline rich region (PRR) mediates binding of SH3 domain-containing proteins, while induced tyrosine phosphorylation sites allow complexes with SH2 domain-containing proteins. These interactions underscore the scaffolding function of the C-terminal sequences in juxtaposing additional targets to Cbl.[9] Targets recruited to Cbl by the TKB domain or the C-terminal interactions are subjected to ubiquitination and negative regulation. From a biochemical standpoint, inhibitors specific to Cbl(TKB) could serve to prevent Cbl recruitment to PTKs and to decouple the PTK binding function from the C-terminal region-mediated scaffolding function.

Several groups have recently identified oncogenic Cbl mutations within the RING and linker regions that are associated with a subset of human myelomonocytic leukemias.[10−14] The mutant Cbl allele is typically duplicated in a copy number-neutral loss of heterozygosity referred to as acquired uniparental disomy (aUPD), which has suggested a potential gain-of-oncogenic function of oncogenic Cbl mutants.[15,16] Clinically relevant Cbl mutations, where analyzed, result in the loss of E3 ligase function but with maintenance of the protein−protein interactions suggesting that E3-deficient oncogenic mutants acquire a scaffolding function to assemble abnormal signaling complexes to promote sustained PTK signaling.[17−20] Since Cbl(TKB) interacts with a large number of PTKs, targeting these enzymes for therapy of cancers driven by Cbl mutations is likely to be limited. On the other hand, a more elegant approach would be to target the mutant Cbl proteins themselves.[21,22] Data from our lab and others suggest that the transforming capacity of Cbl mutants depends on PTK binding; inhibitors of the Cbl(TKB)−PTK interaction could provide a novel means to treat leukemias driven by Cbl(linker/RING) mutations.[21,22,22] The ability to reversibly disrupt the Cbl(TKB)−PTK interaction could also serve as a chemical biological approach to disrupt the function of Cbl proteins and to boost physiological responses in which Cbl proteins play a negative regulatory role.

The systematic development of small molecule inhibitors (SMIs) that perturb protein−protein interactions is becoming more feasible for generating biochemical reagents and therapeutics. From a biochemical standpoint, these compounds can serve as valuable tools to dissect the complex signaling networks in cellular systems. SMIs enjoy several advantages over classical biochemical techniques (i.e., gene knockouts, silencing RNA, mutagenesis). The rapid nature of small molecule inhibition permits the investigation of interactions that occur at much faster time scales, a necessary feature when the real-time responses of cellular pathways are being considered. The tunable nature allows for titrated inhibition,

Received: January 18, 2012
Published: March 6, 2012

   dx.doi.org/10.1021/jm300078z | J. Med. Chem. 2012, 55, 3583−3587

as opposed to the simple on/off mechanism afforded by genetic methods. The reversible nature of small molecule inhibition allows one to disrupt an interaction, observe the response, and end the disruption to recapture the initial condition. Taken together, these attributes offer the ability to directly perturb cellular pathways at the protein level without altering the genetic background of the system. SMIs, therefore, can provide the resolution needed to describe the role of a domain-specific, protein−protein interaction within a given pathway.

RESULTS AND DISCUSSION

In view of the lack of Cbl(TKB) inhibitors and given their biological and clinical relevance, we undertook a peptidomimetic approach. The initial steps in the peptidomimetic design process include (1) identifying a natural ligand, (2) defining the minimal active sequence, and (3) identifying the key residues and their relative 3D arrangement required for activity.[23,24] In this report, we used a combination of methods to identify an optimal Cbl(TKB)-binding lead sequence suitable for structure-guided design. We report an unusual increase in the binding affinity through truncation of a 12-mer Cbl(TKB) binding peptide. We predicted that the pentapeptide (**1**, pYTPEP) and its parental 12-mer peptide (**2**, TLNSDGpYTPEPA) will have similar binding affinity for Cbl. Interestingly, the biochemical data showed that **1** had about 3- to 8-fold higher affinity for Cbl(TKB) compared to **2**. Computational studies with **1** suggest that the N-terminus of the pentapeptide rotates to occupy a shallow groove adjacent to the previously defined binding site. Such an interaction is not feasible with the 12-mer peptide **2**. We propose that this flexibility and reorientation are the source of the improved affinity of **1** compared to **2**. In addition, a library of pentapeptides was used to map the binding interface and define the optimal conformation of the ligand (see Table S1 in Supporting Information for numbering of peptides).

On the basis of the available crystal structures (Figure 1), we generated a truncation peptide set by sequentially removing amino acids from each terminus.[25−27] We started with the 9-mer peptide sequences, as this was the longest sequence in which each residue could be assigned 3D coordinates based on the crystal structures. The truncation set was screened in silico against Cbl(TKB) to identify the smallest unit that retained binding affinity (Table S2). The binding energies were calculated using AutoDock Vina in single calculation mode.[28] Unexpectedly, truncating the peptide to include only the pYTPEP sequence (**1**) resulted in a slight increase in binding affinity. On the basis of this finding, we predicted that the truncated pentapeptide would exhibit comparable binding affinity and provide a reasonable lead compound for a peptidomimetic inhibitor design strategy (Figure S1).

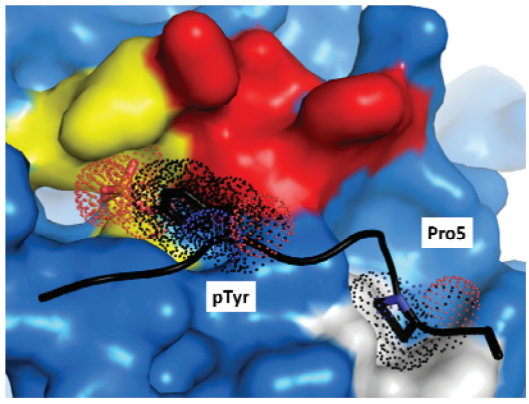

Figure 1. Binding mode of the 12-mer peptide (black cartoon) in complex with Cbl(TKB) (blue surface). The yellow surface represents the pTyr binding site, and the white surface represents the Pro5 binding site. The red surface represents an adjacent binding site. PDB code is 1FBV.

To test this hypothesis, we used a set of orthogonal techniques, viz., fluorescence polarization (FP), isothermal titration calorimetry (ITC), surface plasmon resonance (SPR) (see Supporting Information Table S3 and Figures S2 and S3), and TKB domain pull-down experiments. We recently reported the development and miniaturization of a Cbl(TKB) FP assay for high throughput screening to identify Cbl(TKB) inhibitors.[29] Here, the FP assay was adapted to quantify binding of 12-mer peptide or pentapeptide to Cbl(TKB) and inhibition of binding by various peptides. Peptides **1** and **2** were labeled with a fluorophore at the N-terminus to generate two probes (**3**, Flu-pYTPEP, and **4**, Flu-TLNSDGpYTPEPA) for the FP assay. In two separate experiments, Cbl(TKB) was titrated into a constant concentration of each probe. The K_d values were found to be 2.4 ± 0.1 μM for **3** and 6.2 ± 0.3 μM for **4** (Table 1). These direct binding experiments demonstrated that **3** bound with ∼3-fold better affinity than **4**.

Table 1. Direct and Competitive Binding Experiments with the 12-Mer and Pentapeptides. Thermodynamic Components of Cbl(TKB)−Peptide Binding.[a]

Fluorescence Polarization (FP)			
probe	inhibitor peptide	K_d (μM)	K_i (μM)
flu-short (**3**)		2.4 ± 0.1	
flu-long (**4**)		6.2 ± 0.3	
flu-short (**3**)	**1**		0.8 ± 0.1
flu-short (**3**)	**2**		4.6 ± 0.4
flu-long (**4**)	**1**		0.7 ± 0.3
flu-long (**4**)	**2**		5.5 ± 0.8

Isothermal Titration Calorimetry (ITC)			
peptide	N	K_a ($\times 10^5$) (M^{-1})	ΔG_{ITC} (kcal·mol^{-1})
1	0.93 ± 0.03	14.3 ± 1.6	−8.38 ± 0.03
2	0.93 ± 0.07	2.9 ± 0.5	−7.46 ± 0.04

[a]For FP, the K_i for competitive inhibition was calculated by the Coleska−Wang equation (K_d and K_i, ±SEM).[30] For ITC, ΔG was calculated by the equation $\Delta G = -RT \ln K_a$. The parameters reported are from two separate experiments.

It is feasible that the fluorescent label at the N-terminus of **3** could replace the extended residue sequence of **4** and contribute to the binding affinity. To rule out this possibility, a set of competitive binding experiments were performed where each peptide was titrated vs a constant concentration of Cbl(TKB) and the fluorescently labeled probe. Titration of **1** and **2** vs **3** showed that the unlabeled pentapeptide bound with ∼6-fold better affinity (Table 1). Similarly, titration of **1** and **2** vs **4** showed that the unlabeled pentapeptide bound with ∼8-fold better affinity. As expected, the unlabeled peptides were able to competitively compete for binding with the matched labeled probe and with the unmatched labeled probe. The ability of the pentapeptide to displace the 12-mer probe and vice versa support the hypothesis that **1** occupies the same binding site as **2**. Moreover, the K_i values were comparable

dx.doi.org/10.1021/jm300078z | J. Med. Chem. 2012, 55, 3583−3587

when compared across each probe. That is, the change in probe affinity is accounted for when determining the binding constant for the inhibitor (K_i) in a competitive binding experiment.

Next, ITC was used as an orthogonal technique to directly determine Cbl(TKB)−peptide binding. In separate experiments, **1** and **2** were titrated against a solution of Cbl(TKB) and the heat changes of the solution upon binding were measured. These direct binding experiments demonstrated that the short peptide binds Cbl(TKB) with up to ∼5-fold improvement in the K_a when compared to the long peptide (Table 1). These results are consistent with those observed from the FP measurements.

To determine if the higher affinity of pentapeptide **1** vs the 12-mer **2** can translate into better inhibition of the Cbl(TKB) interaction with an intact cellular binding partner, we conducted pull-down experiments with activated epidermal growth factor receptor (EGFR) expressed in an immortal human mammary epithelial cell line 16A5.[31] In a typical experiment, cells were stimulated with EGF, which results in the phosphorylation of EGFR (pEGFR). GST-Cbl(TKB) fusion protein isolated on glutathione-Sepharose beads was used to pull down activated EGFR from lysates of EGF-stimulated cells in the absence or presence of increasing concentrations of each peptide. After 1 h of incubation, the beads were spun down, and the bound pEGFR protein was visualized using Western blotting for pTyr. The results from the pull-down experiments are summarized in Figure 2. As

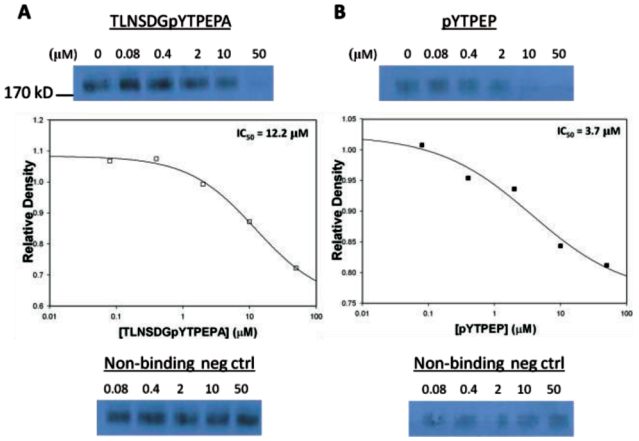

Figure 2. Differential competition of pEGFR pull-down by GST-Cbl(TKB) in the presence of increasing amounts of (A) **2** or (B) **1** assessed using immunoblotting for pEGFR with an anti-phosphotyrosine antibody 4G10. Negative control peptides do not inhibit the Cbl(TKB) pull-down of pEGFR. Band intensities were quantified using Image-J software and pull-down IC_{50} values were determined by nonlinear regression using SigmaPlot.

expected, we observed a decrease in the binding of pEGFR with increasing concentrations of the inhibitor peptides. Moreover, **1** has ∼3-fold better IC_{50} compared to **2**. Together, the biochemical studies clearly show that the computationally predicted pentapeptide **1** binds Cbl(TKB) with about 3- to 8-fold higher affinity compared to the 12-mer peptide **2**.

To identify the key residues required for binding within the pentapeptide **1**, an alanine scan was performed in which each residue was sequentially replaced with an Ala (**15**−**20**) residue. We and others have shown that the phophotyrosine is a key binding component, as the nonphosphorylated Tyr-containing peptide does not bind Cbl(TKB).[6,7,29] Analysis of ΔΔ*G* relative to **1** reveals that each residue modestly contributes to Cbl(TKB) binding (Figure 3A, cyan bars). Interestingly, there

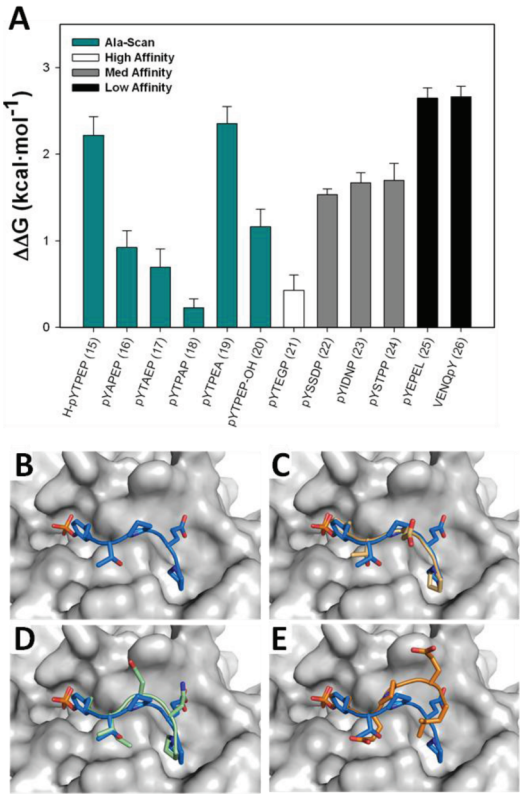

Figure 3. (A) ΔΔ*G* of a focused peptide library of truncated Cbl(TKB) binding peptides. The reported ΔΔ*G* is relative to **1**. K_i was calculated according to the Coleska−Wang equation and $\Delta G = RT \ln K_i$.[30] The reported values were determined from three separate FP experiments. (B−E) Overlaid crystal structures of Cbl-binding peptides illustrating the backbone geometry relative to (B) the highest affinity peptide (**1**, blue), (C) **21** (brown), (D) **23** (green), (E) **25** (orange).

is a significant loss of activity in **19**, suggesting that the proline residue at the P + 4 position makes substantial contribution to binding. Introduction of a carboxylic acid in place of carboxamide on the C-terminal P + 4 proline also results in a loss of activity in **20**, which highlights the hydrophobic nature of the interaction. Taken together, this indicates that **1** is anchored to Cbl(TKB) in a two-point binding fashion. These sites can potentially be exploited to improve inhibition. Furthermore, removal of the acyl group at the N-terminus, in **15**, results in a loss of Δ*G* of ∼2 kcal·mol^{-1}. This change suggested that there is a possible third anchoring interaction.

Several 12-mer peptides have been identified that bind Cbl(TKB), and the crystal structures of many of these complexes have been solved.[25,26] On the basis of these reports and our observations, each known Cbl(TKB)-binding peptide was truncated to the corresponding pentapeptide sequences and tested for binding-inhibitory activity (Figure 3A, white, gray, and black bars). It was observed that those peptides that adopt the same binding mode and orientation as **1** have comparable affinity (**21**, Figure 3C). The peptide orientations that deviate slightly lose activity by ∼1 order of magnitude (**22**−**24**, Figure 3D), and the peptide backbones that deviate significantly from **1** have ∼2 orders of magnitude lower activity (**25** and **26**, Figure 3E). These results suggest that in addition

dx.doi.org/10.1021/jm300078z | J. Med. Chem. 2012, 55, 3583−3587

to the contacts made by the phosphate group and the P + 4 Pro residue, the backbone geometry might contribute to Cbl(TKB) binding.

In parallel, we conducted a computational study to determine binding affinities of the peptides in the library depicted in Figure 3. A plot of the experimentally determined vs the computed binding affinities resulted in an R^2 of 0.68 (Figure 4A). This suggests that at least for this system a docking-guided peptidomimetic inhibitor optimization will be reliable.

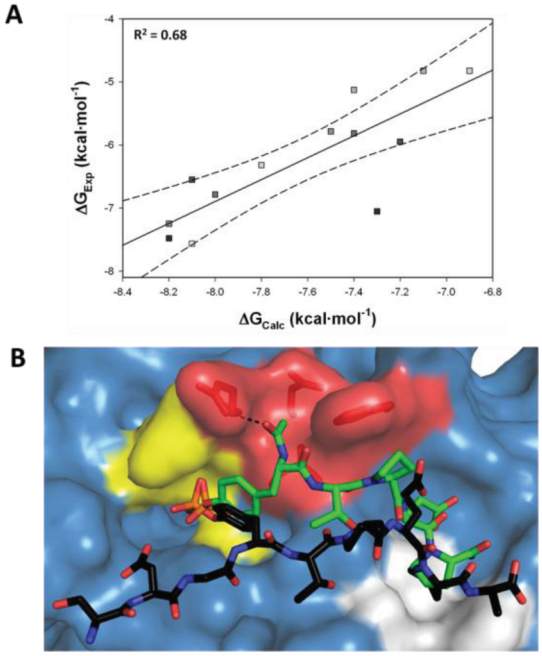

Figure 4. (A) Correlation of binding affinities based on experimental data (ΔG_{Exp}) and docking studies (ΔG_{Calc}). Solid lines represent the best linear fit, and the dashed lines represent the 95% confidence interval. (B) Calculated binding mode of **1** (green sticks) and crystal structure of **2** (black sticks) in complex with Cbl(TKB) (color coordinated as Figure 1). The coordinates for the truncated peptide were generated using a hybrid docking molecular dynamics simulation, and the graphic was generated using PyMOL.[32] PDB code is 1FBV.

On the basis of the fidelity of our computational studies, we were able to determine the most active binding mode of **1** and overlaid the docked structure onto the crystal structure of **2** (Figure 4B and Table S4). The ΔG_{Calc} of the best conformation was -8.2 kcal·mol^{-1}. It was observed that when the residues N terminal to the pTyr are removed, the free acyl group can rotate to occupy a shallow pocket situated adjacent to the pTyr binding site (Figure 4B). The pocket is composed of residues Arg_{299}, Gln_{302}, Ile_{318}, and His_{320} (Figure S1). On the basis of these observations, it seems likely that the N-terminal acyl group of pentapeptide **1** forms a hydrogen bond with the Arg_{299} guanidinium group. The Arg_{299} side chain is at prime interacting distance of 2.82 Å and oriented in the optimum collinear geometry (Figure S1). This observation is consistent with the resulting loss in affinity when the acyl group is removed (Figure 3A, peptide **15**). To test this prediction, the oxygen was replaced with a carbon to disrupt hydrogen bond formation, yielding peptide **27** (Figure S1). ΔG_{Calc} was found to be -7.6 kcal·mol^{-1} ($\Delta\Delta G$ = 0.6 kcal·mol^{-1}). **2** results in a loss of ~1 kcal·mol^{-1} in binding affinity and is sterically inhibited from occupying the shallow pocket. Together our data suggest that the pocket formed by the residues Arg_{299}, Gln_{302}, Ile_{318}, and His_{320} can be exploited to generate inhibitors with higher affinity. This is currently under investigation.

CONCLUSION

We have used tandem computational and experimental approaches to identify the minimal peptide unit capable of binding Cbl(TKB). The computational studies predicted that a pentapeptide (**1**) is sufficient for binding and indicated that it is likely a two-point binding mode. Cell-free assays confirmed the interaction of **1** with Cbl(TKB) in direct binding and competitive inhibition assays. Further, these studies demonstrated that pentapeptide **1** bound with a higher affinity than the 12-mer peptide **2**. A pull-down assay with full length proteins revealed that these peptides could inhibit the Cbl(TKB)−protein interaction and that **1** has ~3-fold better activity than **2**, which is consistent with the cell-free binding assays. A SAR study with a small library of pentapeptides indicated that **1** is the minimal unit and that the backbone geometry is important. In parallel, results from a docking study correlated well with the experimental data for the peptide library. Finally, the predicted binding mode of **1** revealed a third point of interaction adjacent to the binding site of the pTyr residue that can be occupied in the absence of the extended N-terminus of **2**. The additional H-bond and buried surface could contribute to the observed increase in binding affinity of the pentapeptide compared to the 12-mer peptide. We are currently exploiting these observations to develop high affinity Cbl(TKB) inhibitors that will be reported in due course.

ASSOCIATED CONTENT

Supporting Information

Experimental methods, Tables S1−S4, and Figures S1−S6. This material is available free of charge via the Internet at http://pubs.acs.org.

AUTHOR INFORMATION

Corresponding Author

*Phone: (402) 559-3793. E-mail: anatarajan@unmc.edu.

Notes

The authors declare no competing financial interest.

ACKNOWLEDGMENTS

This project was supported in part by NIH Grant T32CA009476 (E.A.K. and N.Y.P.), UNMC Program of Excellence Fellowship (E.A.K.), NCI Eppley Cancer Center Support Grant P30CA036727 (G.E.O.B.), NIGMS Grant P20GM103427 (G.E.O.B.), NIH Grant R01CA127239 (A.N.), and NIH Grants R01 CA105489, R01 CA87986, R01 CA116552, and R01 CA99163 (H.B.).

ABBREVIATIONS USED

Cbl(TKB), casitas B-lineage lymphoma (tyrosine kinase binding domain); PTK, protein tyrosine kinase; FP, fluorescence polarization; PPI, protein−protein interaction; ITC, isothermal titration calorimetry; SAR, structure−activity relationship; EGF, epidermal growth factor; EGFR, epidermal growth factor receptor; pEGFR, phosphoepidermal growth factor receptor

REFERENCES

(1) Acconcia, F.; Sigismund, S.; Polo, S. Ubiquitin in trafficking: the network at work. *Exp. Cell Res.* **2009**, *315*, 1610−1618.

(2) Duan, L.; Reddi, A. L.; Ghosh, A.; Dimri, M.; Band, H. The Cbl family and other ubiquitin ligases: destructive forces in control of antigen receptor signaling. *Immunity* **2004**, *21*, 7−17.

(3) Joazeiro, C. A.; Wing, S. S.; Huang, H.; Leverson, J. D.; Hunter, T.; Liu, Y. C. The tyrosine kinase negative regulator c-Cbl as a RING-type, E2-dependent ubiquitin-protein ligase. *Science* **1999**, *286*, 309−312.

(4) Levkowitz, G.; Waterman, H.; Ettenberg, S. A.; Katz, M.; Tsygankov, A. Y.; Alroy, I.; Lavi, S.; Iwai, K.; Reiss, Y.; Ciechanover, A.; Lipkowitz, S.; Yarden, Y. Ubiquitin ligase activity and tyrosine phosphorylation underlie suppression of growth factor signaling by c-Cbl/Sli-1. *Mol. Cell* **1999**, *4*, 1029−1040.

(5) Peschard, P.; Ishiyama, N.; Lin, T.; Lipkowitz, S.; Park, M. A conserved DpYR motif in the juxtamembrane domain of the Met receptor family forms an atypical c-Cbl/Cbl-b tyrosine kinase binding domain binding site required for suppression of oncogenic activation. *J. Biol. Chem.* **2004**, *279*, 29565−29571.

(6) Lupher, M. L. Jr.; Reedquist, K. A.; Miyake, S.; Langdon, W. Y.; Band, H. A novel phosphotyrosine-binding domain in the N-terminal transforming region of Cbl interacts directly and selectively with ZAP-70 in T cells. *J. Biol. Chem.* **1996**, *271*, 24063−24068.

(7) Lupher, M. L. Jr.; Songyang, Z.; Shoelson, S. E.; Cantley, L. C.; Band, H. The Cbl phosphotyrosine-binding domain selects a D(N/D)XpY motif and binds to the Tyr292 negative regulatory phosphorylation site of ZAP-70. *J. Biol. Chem.* **1997**, *272*, 33140−33144.

(8) Swaminathan, G.; Tsygankov, A. Y. The Cbl family proteins: ring leaders in regulation of cell signaling. *J. Cell. Physiol.* **2006**, *209*, 21−43.

(9) Kurakin, A.; Hoffman, N. G.; Kay, B. K. Molecular recognition properties of the C-terminal Sh3 domain of the Cbl associated protein, Cap. *J. Pept. Res.* **1998**, *52*, 331−337.

(10) Abbas, S.; Rotmans, G.; Lowenberg, B.; Valk, P. J. Exon 8 splice site mutations in the gene encoding the E3-ligase CBL are associated with core binding factor acute myeloid leukemias. *Haematologica* **2008**, *93*, 1595−1597.

(11) Caligiuri, M. A.; Briesewitz, R.; Yu, J.; Wang, L.; Wei, M.; Arnoczky, K. J.; Marburger, T. B.; Wen, J.; Perrotti, D.; Bloomfield, C. D.; Whitman, S. P. Novel c-CBL and CBL-b ubiquitin ligase mutations in human acute myeloid leukemia. *Blood* **2007**, *110*, 1022−1024.

(12) Grand, F. H.; Hidalgo-Curtis, C. E.; Ernst, T.; Zoi, K.; Zoi, C.; McGuire, C.; Kreil, S.; Jones, A.; Score, J.; Metzgeroth, G.; Oscier, D.; Hall, A.; Brandts, C.; Serve, H.; Reiter, A.; Chase, A. J.; Cross, N. C. Frequent CBL mutations associated with 11q acquired uniparental disomy in myeloproliferative neoplasms. *Blood* **2009**, *113*, 6182−6192.

(13) Kales, S. C.; Ryan, P. E.; Nau, M. M.; Lipkowitz, S. Cbl and human myeloid neoplasms: the Cbl oncogene comes of age. *Cancer Res.* **2010**, *70*, 4789−4794.

(14) Loh, M. L.; Sakai, D. S.; Flotho, C.; Kang, M.; Fliegauf, M.; Archambeault, S.; Mullighan, C. G.; Chen, L.; Bergstraesser, E.; Bueso-Ramos, C. E.; Emanuel, P. D.; Hasle, H.; Issa, J. P.; van den Heuvel-Eibrink, M. M.; Locatelli, F.; Stary, J.; Trebo, M.; Wlodarski, M.; Zecca, M.; Shannon, K. M.; Niemeyer, C. M. Mutations in CBL occur frequently in juvenile myelomonocytic leukemia. *Blood* **2009**, *114*, 1859−1863.

(15) Dunbar, A. J.; Gondek, L. P.; O'Keefe, C. L.; Makishima, H.; Rataul, M. S.; Szpurka, H.; Sekeres, M. A.; Wang, X. F.; McDevitt, M. A.; Maciejewski, J. P. 250K single nucleotide polymorphism array karyotyping identifies acquired uniparental disomy and homozygous mutations, including novel missense substitutions of c-Cbl, in myeloid malignancies. *Cancer Res.* **2008**, *68*, 10349−10357.

(16) Sanada, M.; Suzuki, T.; Shih, L. Y.; Otsu, M.; Kato, M.; Yamazaki, S.; Tamura, A.; Honda, H.; Sakata-Yanagimoto, M.; Kumano, K.; Oda, H.; Yamagata, T.; Takita, J.; Gotoh, N.; Nakazaki, K.; Kawamata, N.; Onodera, M.; Nobuyoshi, M.; Hayashi, Y.; Harada, H.; Kurokawa, M.; Chiba, S.; Mori, H.; Ozawa, K.; Omine, M.; Hirai, H.; Nakauchi, H.; Koeffler, H. P.; Ogawa, S. Gain-of-function of mutated C-CBL tumour suppressor in myeloid neoplasms. *Nature* **2009**, *460*, 904−908.

(17) Naramura, M.; Nadeau, S.; Mohapatra, B.; Ahmad, G.; Mukhopadhyay, C.; Sattler, M.; Raja, S. M.; Natarajan, A.; Band, V.; Band, H. Mutant Cbl proteins as oncogenic drivers in myeloproliferative disorders. *Oncotarget* **2011**, *2*, 245−250.

(18) Naramura, M.; Band, V.; Band, H. Indispensable roles of mammalian Cbl family proteins as negative regulators of protein tyrosine kinase signaling: Insights from in vivo models. *Commun. Integr. Biol.* **2011**, *4*, 159−162.

(19) Mosesson, Y.; Mills, G. B.; Yarden, Y. Derailed endocytosis: an emerging feature of cancer. *Nat. Rev. Cancer* **2008**, *8*, 835−850.

(20) Peschard, P.; Park, M. Escape from Cbl-mediated down-regulation: a recurrent theme for oncogenic deregulation of receptor tyrosine kinases. *Cancer Cell* **2003**, *3*, 519−523.

(21) Bonita, D. P.; Miyake, S.; Lupher, M. L. Jr.; Langdon, W. Y.; Band, H. Phosphotyrosine binding domain-dependent upregulation of the platelet-derived growth factor receptor alpha signaling cascade by transforming mutants of Cbl: implications for Cbl's function and oncogenicity. *Mol. Cell. Biol.* **1997**, *17*, 4597−4610.

(22) Ogawa, S.; Shih, L. Y.; Suzuki, T.; Otsu, M.; Nakauchi, H.; Koeffler, H. P.; Sanada, M. Deregulated intracellular signaling by mutated c-CBL in myeloid neoplasms. *Clin. Cancer Res.* **2010**, *16*, 3825−3831.

(23) London, N.; Movshovitz-Attias, D.; Schueler-Furman, O. The structural basis of peptide-protein binding strategies. *Structure* **2010**, *18*, 188−199.

(24) Vagner, J.; Qu, H.; Hruby, V. J. Peptidomimetics, a synthetic tool of drug discovery. *Curr. Opin. Chem. Biol.* **2008**, *12*, 292−296.

(25) Meng, W.; Sawasdikosol, S.; Burakoff, S. J.; Eck, M. J. Structure of the amino-terminal domain of Cbl complexed to its binding site on ZAP-70 kinase. *Nature* **1999**, *398*, 84−90.

(26) Ng, C.; Jackson, R. A.; Buschdorf, J. P.; Sun, Q.; Guy, G. R.; Sivaraman, J. Structural basis for a novel intrapeptidyl H-bond and reverse binding of c-Cbl-TKB domain substrates. *EMBO J.* **2008**, *27*, 804−816.

(27) Hu, J.; Hubbard, S. R. Structural characterization of a novel Cbl phosphotyrosine recognition motif in the APS family of adapter proteins. *J. Biol. Chem.* **2005**, *280*, 18943−18949.

(28) Trott, O.; Olson, A. J. AutoDock Vina: improving the speed and accuracy of docking with a new scoring function, efficient optimization, and multithreading. *J. Comput. Chem.* **2010**, *31*, 455−461.

(29) Kumar, E. A.; Charvet, C. D.; Lokesh, G. L.; Natarajan, A. High-throughput fluorescence polarization assay to identify inhibitors of Cbl(TKB)−protein tyrosine kinase interactions. *Anal. Biochem.* **2011**, *411*, 254−260.

(30) Nikolovska-Coleska, Z.; Wang, R.; Fang, X.; Pan, H.; Tomita, Y.; Li, P.; Roller, P. P.; Krajewski, K.; Saito, N. G.; Stuckey, J. A.; Wang, S. Development and optimization of a binding assay for the XIAP BIR3 domain using fluorescence polarization. *Anal. Biochem.* **2004**, *332*, 261−273.

(31) Dimri, M.; Naramura, M.; Duan, L.; Chen, J.; Ortega-Cava, C.; Chen, G.; Goswami, R.; Fernandes, N.; Gao, Q.; Dimri, G. P.; Band, V.; Band, H. Modeling breast cancer-associated c-Src and EGFR overexpression in human MECs: c-Src and EGFR cooperatively promote aberrant three-dimensional acinar structure and invasive behavior. *Cancer Res.* **2007**, *67*, 4164−4172.

(32) Delano, W. L. *PyMOL User's Guide*; Delano Scientific LLC: San Carlos, CA, 2004.